0026-895X/95/061133-08$3.00/0

MOLECULAR PHARMACOLOGY, 47:1133–1140 (1995).

Alternatively Spliced Forms of the α Subunit of the Epithelial Sodium Channel: Distinct Sites for Amiloride Binding and Channel Pore

XIAO-JIANG LI, RUO-HUI XU, WILLIAM B. GUGGINO, and SOLOMON H. SNYDER

Departments of Neuroscience, Psychiatry, and Behavioral Sciences (X.-J.L., S.H.S.), Pharmacology and Molecular Sciences (R.-H.X., S.H.S.), and Physiology (W.B.G.), Johns Hopkins University School of Medicine, Baltimore, Maryland 21205

Received January 9, 1995; Accepted March 23, 1995

SUMMARY

The amiloride-sensitive epithelial sodium channel (ENAC) consists of at least three subunits, α, β, and γ. Sodium conductance occurs when only the α subunit is expressed in *Xenopus* oocytes, but it is greatly enhanced by coexpression of all three subunits. All three subunits have two transmembrane domains. Whether the amiloride binding site exists in the extracellular portion or a transmembrane domain has not been established. Using reverse transcription-polymerase chain reaction in rat taste tissues, we have identified two alternatively spliced transcripts of ENAC (αENACa and αENACb) with deletions of nucleotides that introduce a premature stop codon and may result in proteins shortened by 199 and 216 amino acids, respectively, at the carboxyl terminus. Genomic Southern blots indicate that a single gene accounts for αENAC and the alternatively spliced variants. Reverse transcription-polymerase chain reaction and RNase protection assays demonstrate that αENACa is expressed to a lesser extent than αENAC in kidney, lung, and taste tissues. αENACa differs from αENAC by a deletion in the second transmembrane domain. Despite this deletion, αENACa expression in transfected human embryonic kidney 293 cells or CV-1 cells augments [^{3}H]phenamil binding. The [^{3}H]phenamil binding of αENACa resembles that of αENAC, being inhibited more potently by phenamil (K_d = 65 nM) than amiloride. Unlike αENAC, expression of αENACa in *Xenopus* oocytes fails to generate amiloride-sensitive Na^+ or Li^+ currents. These results suggest that the amiloride binding site resides on the extracellular loop of the α subunit of ENAC and not the putative second transmembrane domain, which forms a channel pore. Heterogeneity in αENAC isoforms may contribute to the complexity of multimeric structures and functional variation of ENAC.

Active sodium reabsorption by epithelia throughout the body, including kidney tubules, the distal colon, and sweat and salivary glands, is mediated by ENAC (1). These channels are primarily characterized by their selective high affinity for the diuretic amiloride. Salty taste also appears to involve ENAC, because amiloride can reduce salt taste transduction and human salt perception (2–4). ENAC has been purified from kidney as a large protein complex (5, 6). Recent molecular cloning studies indicate that ENAC consists of at least three subunits (α, β, and γ), each of which possesses two transmembrane domains (7–9). The αENAC confers a low amplitude, amiloride-sensitive, sodium current, whereas β and γ subunits are required for maximal channel activity. We localized αENAC to discrete areas of the epithelia of the lung and colon as well as the tongue, with a disposition that can account for salty taste perception (10). In the present study we examined the potential heterogeneity of αENAC in various tissues using RT-PCR. We now report two alternatively spliced forms of αENAC, αENACa and αENACb. Utilizing expressed αENACa and αENAC in mammalian cells and *Xenopus* oocytes, we obtained evidence that amiloride binding and channel conductance are mediated by distinct domains.

Materials and Methods

RT-PCR. Ten micrograms of total RNA from various tissues were reverse transcribed using 1 μg of oligo(dT) as primer in a 50-μl reaction, which contained 500 μM deoxynucleotide triphosphates, 50 units of RNase (Boehringer Mannheim), 200 units of Moloney murine leukemia virus reverse transcriptase (BRL), and a buffer of 50 mM Tris, pH 8.3, 50 mM KCl, 8 mM $MgCl_2$, and 10 mM dithiothreitol. One microliter of the reverse transcriptase mixture was used in a 25-μl PCR mixture containing 1.5 mM $MgCl_2$, 400 nM primers, 200 μM deoxynucleotide triphosphates, and 0.5 unit of *Thermus aquaticus* polymerase (Boehringer Mannheim). To identify homologues of αENAC, two degenerate oligonucleotides that correspond to se-

ABBREVIATIONS: ENAC, amiloride-sensitive epithelial sodium channel(s); αENAC, α subunit of amiloride-sensitive epithelial sodium channel(s); RT, reverse transcription; PCR, polymerase chain reaction; kb, kilobase(s); HEK, human embryonic kidney; mAb, monoclonal antibody; HEPES, 4-(2-hydroxyethyl)-1-piperazineethanesulfonic acid; PIPES, piperazine-*N*,*N*′-bis(2-ethanesulfonic acid); SSC, standard saline citrate.

quences conserved between rat αENAC and *Caenorhabditis elegans* degenerins proteins Mec-4 and Deg-1 (7, 8) were used as primers for RT-PCR. αEN-S3 [CAGGT(G/C)GAATTC(A/G)(C/T)TC(A/C/T)TG(C/T)TT(T/C)CA] is the forward primer and corresponds to the αENAC amino acid sequence CIHSCFQ (residues 443–449); αEN-A3 [GATCCACTCGAGNGA(T/C)TTNACNGANGGCCA] is the reverse primer and corresponds to the αENAC amino acid sequence WPSVKS (residues 520–525). PCR conditions were 35 cycles of 1 min at 95°, 2 min at 45°, and 1 min at 72°. The PCR product was visualized on a 1.5% agarose gel, and the band corresponding to the expected size was subcloned and sequenced.

To determine whether alternatively spliced variants possess the same sequences in the amino and carboxyl termini as does αENAC, specific oligonucleotides were used for the amplification of cDNA prepared from different tissues. The antisense primers αEN-A1 (TTATAATAGCAATAGCCCCA) for αENAC and αENa-A1 (TCCAAGGAGAAGGCGCCCCCA) for αENACa were used with the oligonucleotide (S1) encoding the amino-terminal sequence (GAGGGCAGCCTGGGATGCGG) to amplify cDNA encoding the amino-terminal region of the protein. The sense primers αEN-S2 (CAGAGCTCCTGGGGCTATTG) for αENAC and αENa-S2 (CAGAGCTCCTGGGGGCGCCTT) for αENACa were used with an antisense oligonucleotide (A2) encoding the carboxyl-terminal sequence (CTTGAATTCTCTCAGAGCGCC) to amplify products encoding the carboxyl-terminal portion of this channel. First-strand cDNAs were prepared from taste tissues, lung, and kidney. PCR products from taste tissues and lung that were obtained with specific primers for αENACa were subcloned into the pCR-II vector (Invitrogen) and sequenced. RNA was also prepared from HEK-293 cells transfected with αENAC or the alternatively spliced form αENACa, to serve as templates for RT-PCR analysis of the specificity of the oligonucleotide primers. PCR was conducted under the same conditions as described above, except that the annealing temperature was 65°. The PCR products were separated in 1% agarose gels, transferred to nitrocellulose membranes, and hybridized with the entire cDNA fragment (3 kb) of αENAC, which was labeled with ^{32}P. The PCR Southern blot was conducted under high stringency (50% formamide/5× SSC at 42° for hybridization and 1× SSC at 65° for a final wash), and blots were exposed to X-ray film.

RNase protection assay and genomic DNA Southern blot analysis. In the RNase protection assay, the alternatively spliced cDNA clone αENACa identified by PCR using primers αEN-S3 and αEN-A3 was used to generate a [^{32}P]UTP-labeled antisense RNA probe, using T3 RNA polymerase. Twenty micrograms of total RNA from various tissues were hybridized with the antisense RNA probe (1×10^5 cpm) in 20 μl of reaction buffer (80% formamide, 40 mM PIPES, pH 6.4, 400 mM sodium acetate, pH 6.4, 1 mM EDTA) at 55° for 18 hr. RNase A and RNase T1 (1/100 dilution) were then used to digest unprotected RNA, following the instructions for the RNase protection assay kit (Ambion). The protected pieces of RNA probes were fractionated on a 5% acrylamide gel and visualized by exposure to Kodak X-ray film for 4 days.

Genomic DNA was prepared from rat testis using standard procedures. Five micrograms of DNA were digested with *Eco*RI, *Hind*III, *Bam*HI, and *Xba*I. The digested DNA was then fractionated in 0.7% agarose gels and blotted onto nitrocellulose membranes. The αENACa cDNA product (223 base pairs) generated by PCR primers αEN-S3 and αEN-A3 was labeled with ^{32}P using a random primer kit. Hybridization and washing were carried out under moderate stringency (6× SSC at 55°, with a wash with 2× SSC at 50°). The blot was exposed to X-ray film for 4 days.

Transfection of DNA in mammalian cells and [^{3}H]phenamil binding assay. The full length cDNA of αENAC obtained by screening of a rat taste cDNA library (10) was cut with *Not*I and *Xho*I and inserted into the expression vector pCIS. The PCR product of the alternatively spliced form αENACa was cut with *Bcl*I to replace the corresponding region of αENAC in pCIS. We used a PCR primer (CCATCGATGGCCACCATGGAACAAAAACTTATTAGTGAAGAAGATCTTGGATCCATGCTGGACCACAGGA) that contains a *Bam*HI digestion site so that we could insert the sequence for the epitope of c-Myc (MEQKLSEEDL), followed by two additional amino acids (GS), into the amino terminus of both αENAC and αENACa cDNA. mAbs against c-Myc were then used to evaluate the protein expression of those constructs in transfected cells. Thus, we constructed αENAC and αENACa in the expression vector for transient expression in mammalian cells. DNA (10 μg) was then transfected into HEK-293 cells and CV-1 cells (an African green monkey kidney cell line) by the calcium phosphate technique. After 48–72 hr, transfected cells were washed once with phosphate-buffered saline and collected for immunoblot and ligand binding assays.

Immunoblot assays were conducted using proteins from transfected HEK-293 cells and a mAb specific for c-Myc (11). The whole-cell proteins (100 μg) were resolved in 4–12% gradient sodium dodecyl sulfate-acrylamide gels and transferred to nitrocellulose membranes. The blots were incubated in phosphate-buffered saline containing c-Myc-specific mAb (1/5000) and 5% nonfat milk, and recognized proteins were visualized using the enhanced chemiluminescence detection assay (Amersham).

[^{3}H]Phenamil (2.8 Ci/mmol), an amiloride analogue, was synthesized by NEN-DuPont as a custom preparation. Transfected HEK-293 or CV-1 cells were harvested in cold (4°) binding buffer containing 1 mM EDTA, 15 mM Tris·HCl, pH 7.7, 1 μM pepstatin A, 0.1 μM aprotinin, 0.1 mM phenylmethylsulfonyl fluoride, and 10 μM leupeptin. Cells were then homogenized and centrifuged, and the pellet was resuspended in the binding buffer at a concentration of 1–2 mg/ml. The reaction mixture (0.2 ml), containing [^{3}H]phenamil and 100 μg of protein, was incubated at 4° for 90 min, and the reaction was terminated by rapid filtration through Whatman GF/B glass fiber filters that had been pretreated with 0.3% polyethyleneimine. Phenamil (Research Biochemicals International) and amiloride (Sigma), suspended in dimethylformamide, were used as competitors in the binding assay. Protein was assayed by using a kit (Pierce), with bovine serum albumin as a standard.

Expression of cDNA in *Xenopus* oocytes. cDNA for β and γ subunits of ENAC was isolated from rat lung by PCR. These cDNAs, as well as cDNA for αENAC and αENACa, were subcloned into pCDNA-III (Invitrogen), and capped cRNA was synthesized using T7 RNA polymerase with a cRNA synthesis kit (Ambion). cRNA for αENAC or αENACa was coinjected with β and γ subunit cRNA into *Xenopus* oocytes (about 10 ng of cRNA for each subunit). At 48 hr after injection, the oocytes were clamped at −100 mV and amiloride-sensitive currents were measured by determining the difference in current before and after addition of 5 μM amiloride in the bath. The bath solution contained 100 mM sodium gluconate, 2 mM KCl, 1.8 mM $CaCl_2$, and 10 mM HEPES, pH 7.2, as well as the K^+ channel blockers barium (5 mM) and tetraethylammonium (10 mM). Current-voltage curves were obtained by setting the command potential for 1 sec (at 4-sec intervals) from a −100-mV holding potential to values ranging from +40 to −140 mV.

Results

Identification of alternatively spliced forms of αENAC. The sole form of αENAC cloned from epithelial tissues of mammalian species displays substantial homology to mechanosensitive proteins associated with degeneration of neurons that mediate touch sensitivity in *C. elegans* (7, 8). To search for homologues of αENAC, we constructed degenerate primers based on regions that are conserved between the mechanosensitive proteins of *C. elegans* and αENAC (Fig. 1a). These primers give rise to several PCR products (246, 223, and 167 bases). In one of the PCR products, αENACa (223 bases), we identified a deletion of 23 bases, whereas the rest of the sequence is identical to αENAC. The deletion

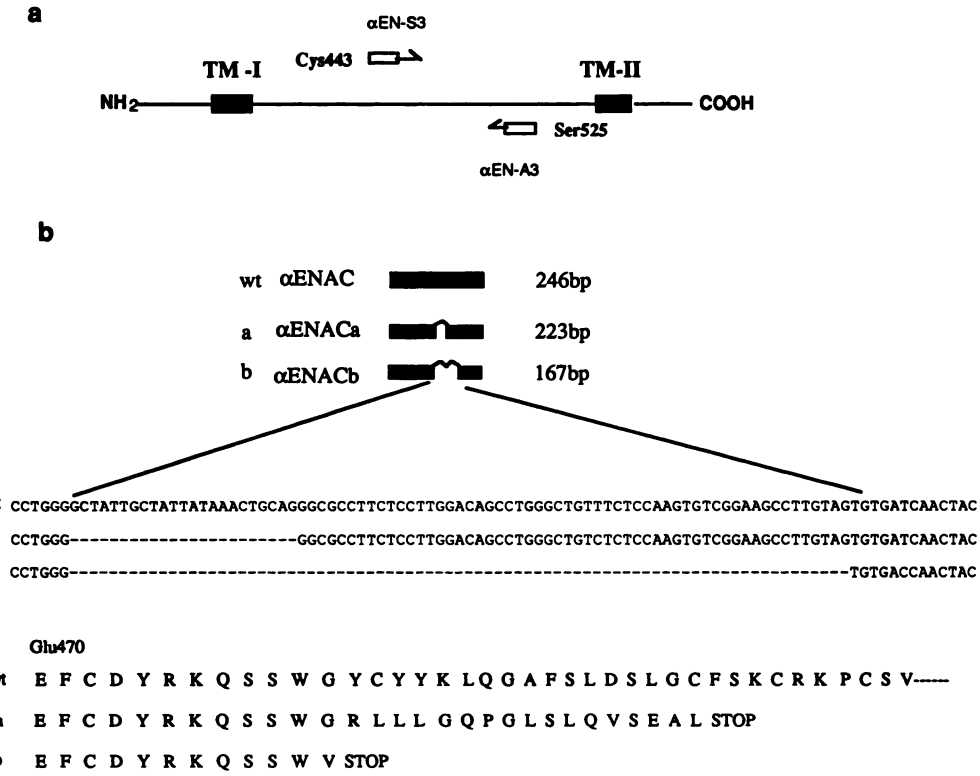

Fig. 1. Identification by RT-PCR of alternatively spliced transcripts from rat taste tissues. a, Degenerate sense (αEN-S3) and antisense (αEN-A3) oligonucleotides were used to amplify cDNA made from rat circumvallate papillae tissue containing taste cells. The indicated PCR products, which encode a portion of protein between two putative transmembrane (*TM*) domains (*black boxes*), were obtained. b, Sequence analysis of PCR products (αENAC, αENACa, and αENACb) showed that 23 bases and 79 bases (*space between black boxes*) have been deleted in αENACa and αENACb, respectively, with subsequent insertion of a premature stop codon. The two alternatively spliced transcripts share the same splicing site (CTCCTGGG). *wt*, wild-type αENAC; *a*, alternatively spliced form αENACa; *b*, alternatively spliced form αENACb.

occurs between bases TCCTGGG and GGCGCCT and is associated with a reading frame shift that results in a sequence change of 17 amino acids, followed by a stop codon. Another PCR product, αENACb, shows a 79-base deletion that starts with the same splicing site (TCCTGGG) as αENACa; a premature stop codon immediately follows the splicing site (Fig. 1b). These premature stop codons generate deletions of 199 or 216 amino acids, respectively, at the carboxyl terminus in αENAC, which may result in shorter proteins with 499 or 482 amino acids, respectively, compared with the expected αENAC protein (698 amino acids).

Genomic Southern analysis of αENAC. To ascertain whether alternatively spliced transcripts for αENAC are derived from a single gene or from multiple genes, we conducted genomic Southern blot analysis using a probe comprising a 223-base PCR product obtained from αENACa (Fig. 2). We observe a single major hybridization band in the digests of genomic DNA with *Eco*RI (9.5 kb), *Hind*III (2.5 kb), *Bam*HI (7 kb), or *Xba*I (9 kb). With *Hind*III two minor bands at 4.5 and 8 kb are evident but are not observed consistently in repeated experiments. Because αENACa differs from αENAC only in a 23-base deletion, it should hybridize to genes for native and alternatively spliced forms of the channel. Accordingly, the existence of one band indicates that a single gene accounts for αENAC and αENACa.

Comparison of αENAC and its alternatively spliced forms using RT-PCR. The two alternatively spliced variants share the same splicing start site and generate similar truncated proteins. We further characterized the splicing variant αENACa. To ascertain whether αENACa possesses the same sequence as αENAC except for the 23-base deletion, we conducted PCR analysis using primers selective for αENACa or αENAC (Fig. 3). The specificity of those primers was verified by RT-PCR with RNA prepared from HEK-293 cells transfected with either αENAC or αENACa cDNA. Using a sense or antisense primer specific for αENAC along with a primer selective for the carboxyl-terminal or amino-terminal portion of αENAC, we detect a signal in the cells transfected with αENAC but not in cells transfected with αENACa. In contrast, using primers selective for αENACa, we detect a signal only in cells transfected with αENACa and not in those transfected with αENAC. PCR products obtained from different tissues using primers for αENACa display the same size as do those obtained with primers for αENAC. cDNA sequence analysis of these PCR products indicates that, except for the deletion, the two forms of αENAC possess identical sequences. In contrast to results with αENACa, we have failed to obtain the amino-terminal sequence of αENACb using RT-PCR, despite repeated attempts. Conceivably, transcript expression is much lower for αENACb than αENACa.

As reported previously, αENAC mRNA is highly expressed in lung, kidney, and tongue but not in brain (10). Using primers for the carboxyl-terminal portion of the channel, we have confirmed the similar relative levels of αENAC in taste bud-enriched tissue and in epithelium obtained from the entire tongue (Fig. 3, A and B). PCR signals for αENACa are substantially lower than those for αENAC. In contrast to

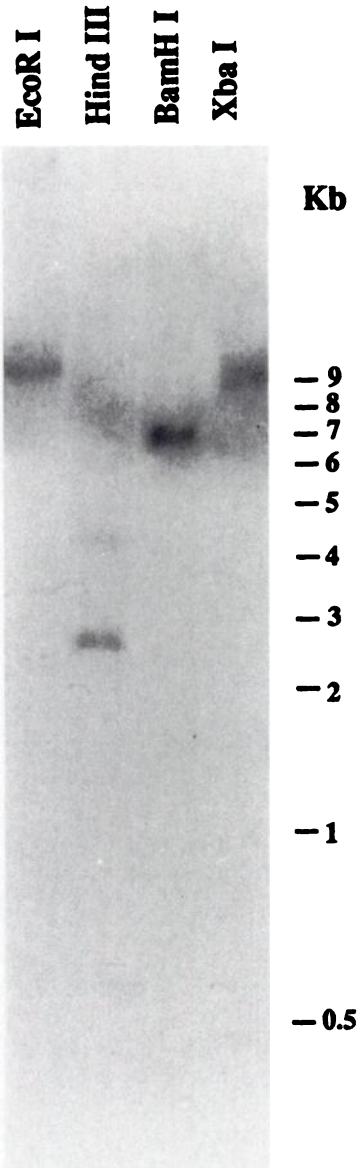

Fig. 2. Genomic Southern blot analysis of the rat αENAC gene. Five micrograms of rat testis genomic DNA were digested with the enzymes *Eco*RI, *Hind*III, *Bam*HI, and *Xba*I, fractionated in a 0.7% agarose gel, and hybridized to a ^{32}P-labeled cDNA probe generated from the alternatively spliced, PCR product αENACa (223 base pairs), under moderate stringency hybridization, as described in Materials and Methods.

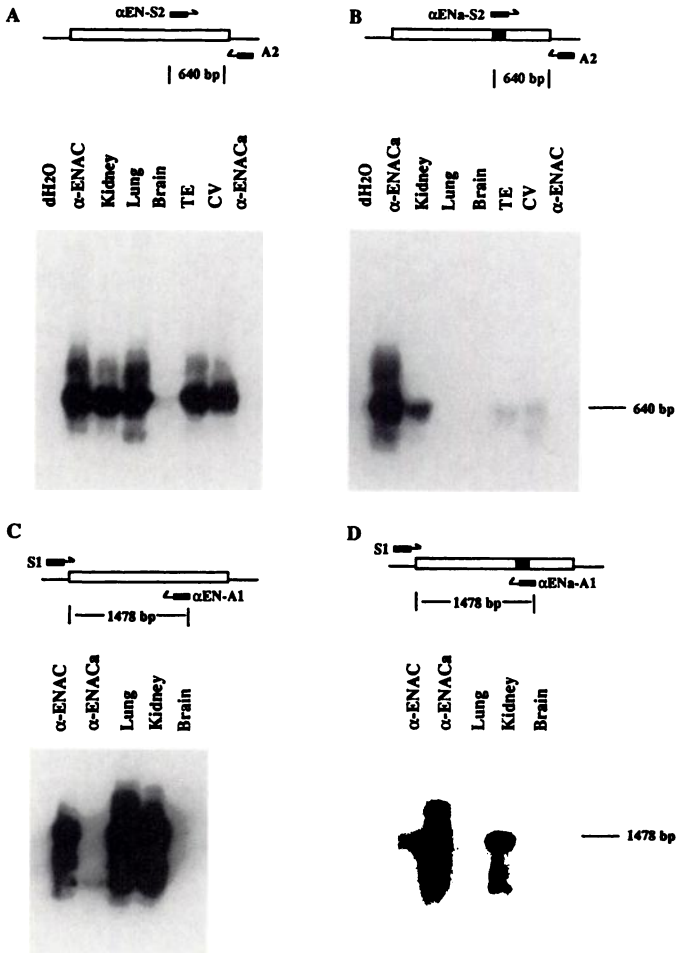

Fig. 3. RT-PCR analysis of RNA expression of αENAC and the alternatively spliced form αENACa. Specific primers for αENAC and its alternatively spliced form αENACa (see Materials and Methods) were used to amplify cDNAs prepared from different tissues. A and B, Amplification with specific sense primers and carboxyl-terminal primers; C and D, amplification with specific antisense primers and amino-terminal primers. *dH$_2$O*, water without cDNA template; *α-ENAC* and *α-ENACa*, HEK-293 cells transfected with αENAC and alternatively spliced form αENACa cDNA, respectively; *TE*, rat tongue epithelia; *CV*, tongue taste tissue enriched in circumvallate papillae. The sizes of expected PCR products are indicated.

αENAC, αENACa expression is undetectable in the lung, although substantial signals are evident for kidney and tongue. As with αENAC, αENACa is not detected in the brain. We also conducted PCR analysis using a primer selective for the amino-terminal portion of αENAC along with an antisense primer, from the mid-region of the channel, selective for either αENAC or αENACa (Fig. 3, C and D). The results from kidney and lung confirm the findings obtained with the primers directed toward the carboxyl-terminal region. Thus, analysis of the amino-terminal portion of the protein with primers selective for αENAC reveals comparable expression in the lung and kidney, whereas with αENACa-selective primers expression is less in the kidney and undetectable in the lung.

Tissue distribution of two forms of αENAC analyzed by RNase protection analysis. Quantification of relative amounts of RNA is difficult with PCR technology. Because alternative splicing results in a deletion of <23 nucleotide base pairs, it is also difficult to distinguish the transcripts for αENAC and αENACa using Northern blot analysis or *in situ* hybridization. Thus, we conducted RNase protection analysis using an RNA probe derived from a PCR clone for αENACa, to verify the tissue distribution of αENACa and αENAC (Fig. 4). The protected band of 201 nucleotides represents alternatively spliced transcripts of αENACa, whereas protected bands of 99–105 nucleotides reflect transcripts of αENAC that have been digested by RNase. As observed in PCR analysis, levels of αENAC transcripts (99–105 nucleotides) are substantially higher than those of αENACa transcripts (201 nucleotides). The highest densities of αENAC transcripts are observed in lung and kidney, with levels in kidney being somewhat higher than those in lung. Substantial and similar levels occur in epithelial tissue of the tongue and in taste bud-enriched tissue. No expression of αENAC is observed in

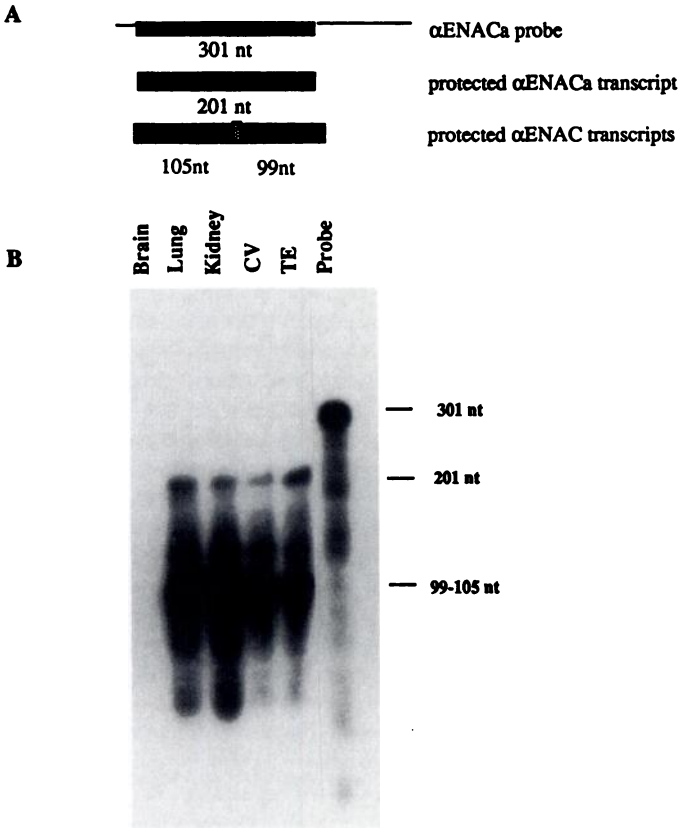

Fig. 4. RNase protection analysis of alternatively spliced αENACa in various rat tissues. Twenty micrograms of total RNA from rat brain, lung, kidney, tongue circumvallate papillae (*CV*), and tongue epithelial tissue adjacent to circumvallate papillae (*TE*) were hybridized to a ^{32}P-labeled antisense RNA probe (310 nucleotides) transcribed from a Bluescript plasmid containing alternatively spliced cDNA αENACa fragment (201 nucleotides) (*black box*). The protected size (201 nucleotides) of transcripts for αENACa and the expected sizes (99 and 105 nucleotides) of transcripts for αENAC digested by RNase are indicated. The additional protected size suggests the existence of other alternatively spliced forms or RNA degradation.

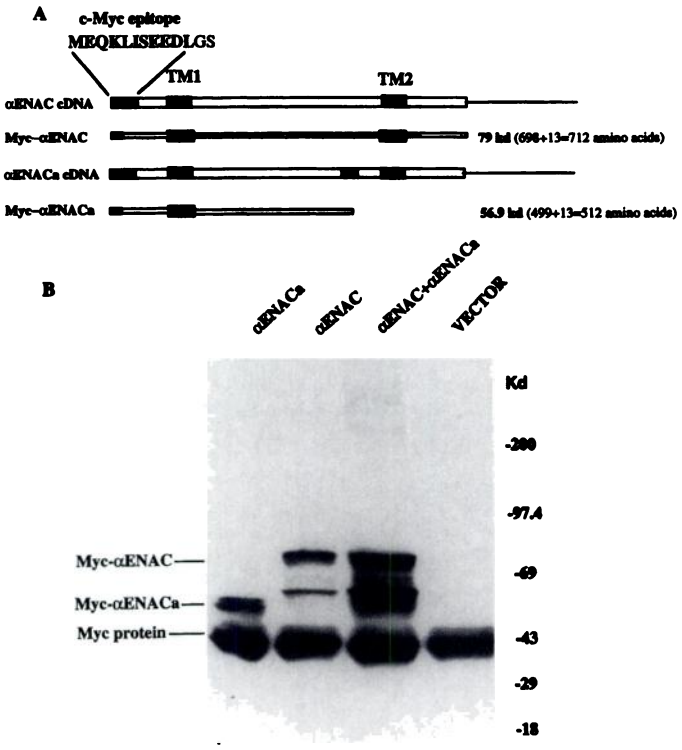

Fig. 5. Immunoblot of expressed αENAC and αENACa in HEK-293 cells. A, The insertion of the 13 amino acids containing the c-Myc epitope (MEQKLISEEDL) and the two amino acids GS into the amino terminus of αENAC and αENACa was made in the mammalian expression vector pCIS. These constructs were expressed by transient transfection in HEK-293 cells; the expected molecular masses of αENAC and αENACa are 79 kDa and 56.9 kDa, respectively. B, αENAC or αENACa with c-Myc epitope expressed in HEK-293 cells is recognized by anti-Myc mAb. Cells were transfected with αENACa, with αENAC, with αENACa and αENAC, and with the pCIS vector. The endogenous c-Myc protein in HEK-293 cells recognized by anti-Myc mAb reflects equal amounts of total proteins in each lane.

brain. RNase protection reveals a protected size of 201 nucleotides for αENACa transcripts. αENACa levels in epithelial tissue of the tongue are slightly higher than those in taste bud-enriched regions. As in PCR experiments, RNase analysis reveals no expression of αENACa in the brain. αENACa levels are comparable in lung and in kidney, in contrast to PCR analysis, which reveals no expression in lung. The RNase assay also reveals additional sizes of protected transcripts, which could reflect either other alternative splicing in this region, as observed for αENACb, or RNA degradation.

Immunoblot assay of expressed αENAC and αENACa in HEK-293 cells. By tagging the c-Myc epitope on the amino terminus of αENAC and αENACa, we detect transfected proteins in HEK-293 cells. The alternatively spliced form αENACa gives rise to a smaller truncated protein when expressed in HEK-293 cells, as expected from its alternatively spliced region (Fig. 5). The truncated protein of 56.9 kDa, which is shorter than αENAC (79 kDa), results from a premature stop codon that causes a deletion of 199 amino acids, including the putative second transmembrane domain. Repeated experiments using endogenous c-Myc protein for evaluation of total amounts of sample protein loaded in the gel show comparable expression levels for αENAC and αENACa in transfected cells, and coexpression of both proteins does not significantly affect the expression level of each protein.

Ligand binding in transfected cells. ENAC has been extensively characterized in intact tissues by the binding of radioactive ligands. Of those used, [^{3}H]phenamil possesses the highest affinity for the channel and has provided the most abundant and selective binding. Previous studies reporting the cloning of αENAC verified its physiological significance by demonstrating electrical conductance of ENAC in oocytes injected with αENAC cRNA (7–9). Ligand binding to αENAC was not reported. HEK-293 cells were previously used for expression of cDNA for an amiloride-binding protein (12). We evaluated [^{3}H]phenamil binding in HEK-293 cells as well as CV-1 cells transfected with αENAC or the alternatively spliced form αENACa. Untransfected cells display substantial [^{3}H]phenamil binding. We also evaluated COS-1 and BALB/3T3 cells, both of which display similar endogenous levels of [^{3}H]phenamil binding. [^{3}H]Phenamil binding is 2.5–3-fold greater in cells transfected with αENAC or αENACa than in cells transfected only with the expression vector (Fig. 6A). Saturation analysis involving a range of [^{3}H]phenamil concentrations also establishes that binding is higher in αENAC-transfected (B_{max} = 8.2 pmol/mg of protein) and

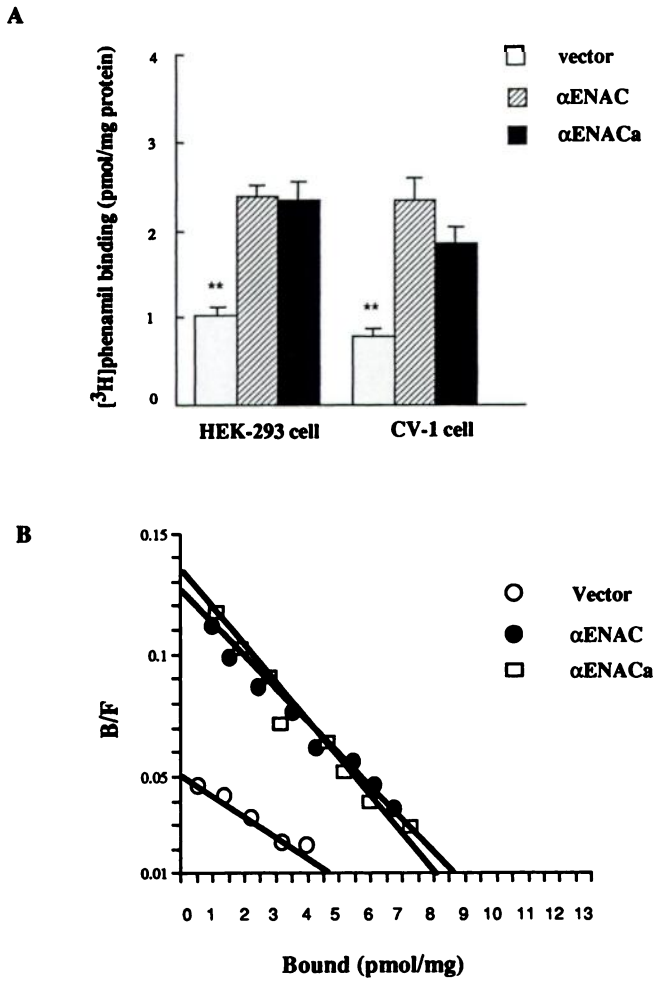

Fig. 6. [^{3}H]Phenamil binding in transfected HEK-293 or CV-1 cells. A, Comparison of binding of [^{3}H]phenamil to HEK-293 and CV-1 cells transfected with αENACa or αENAC. Concentrations of [^{3}H]phenamil and phenamil were 50 nM and 0.1 mM, respectively. Results were obtained from three or four independent transfection experiments. **, $p < 0.01$ for values from control cells, compared with those from αENAC- or αENACa-transfected cells. B, Scatchard plots of [^{3}H]phenamil binding to transfected cells. Nonspecific binding was assayed in the presence of unlabeled phenamil (0.1 mM). Each *point* represents results from two experiments.

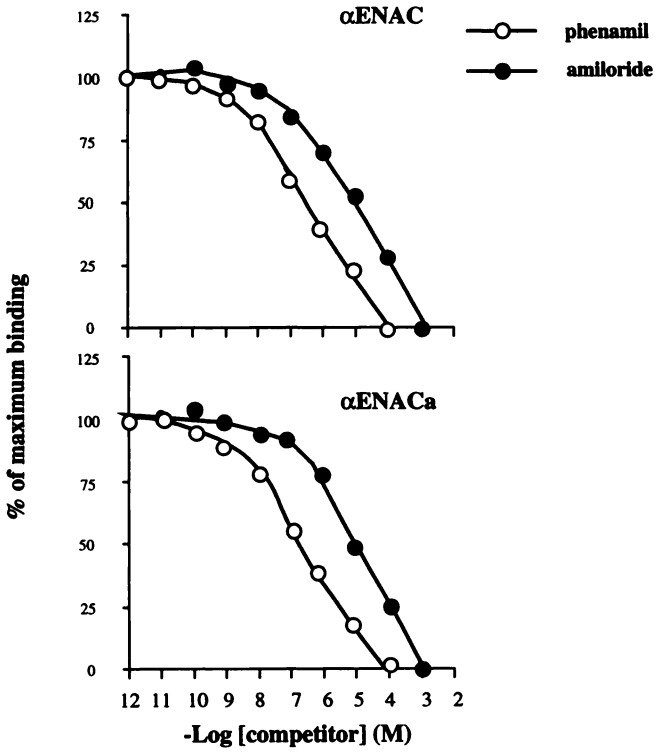

Fig. 7. Inhibition by various concentrations of phenamil and amiloride of binding of [^{3}H]phenamil to HEK-293 cells transfected with αENACa or αENAC. Membrane protein (100 μg) was incubated with 50 nM [^{3}H]phenamil in the absence or presence of increasing concentrations of competitors. Two independent experiments were performed in duplicate. Results are presented for a typical experiment, with values varying <20%.

αENACa-transfected (B_{max} = 8.6 pmol/mg of protein) cells than in those transfected with vector alone (B_{max} = 4.5 pmol/mg of protein) (Fig. 6B). The binding affinity for phenamil in αENACa- and αENAC-transfected cells (K_d = 65 nM) is comparable to that of the native ENAC in intact tissues (K_d = 20–30 nM) (13, 14). The binding affinity for [^{3}H]phenamil (K_d = 82 nM) in 293 cells transfected with vector only is indistinguishable from the affinity (K_d = 65 nM) in cells transfected with αENAC or αENACa. Both control cells and αENAC- or αENACa-transfected cells appear to have a single component of [^{3}H]phenamil binding. Phenamil is about 100 times more potent than amiloride in competing for [^{3}H]phenamil binding in cells transfected with αENACa or αENAC (Fig. 7). The IC_{50} (100 nM) for phenamil competion with [^{3}H]phenamil binding in transfected cells expressing αENAC or αENACa is similar to that (IC_{50} = 44 nM) for inhibition of Na^+ currents in *Xenopus* oocytes expressing cloned rat αENAC (8).

Expression in *Xenopus* oocytes. Coexpression of α, β, and γ subunits of ENAC in *Xenopus* oocytes induced large and highly selective Na^+ and Li^+ inward currents (9). To compare the channel activities of αENACa and αENAC, we injected cRNA for αENACa or αENAC, with β and γ subunit cRNAs, into *Xenopus* oocytes (Fig. 8). The αENAC with β and γ subunits expressed in oocytes produces large, amiloride-sensitive, Na^+ and Li^+ inward currents. The Li^+ current is about twice as large as the Na^+ current. The properties of αENAC we observe are consistent with a previous report (9). Even with coexpression of β and γ subunits, the alternatively spliced form αENACa does not generate amiloride-sensitive Na^+ or Li^+ currents. Oocytes injected with αENACa display the same electrophysiological behavior as do oocytes injected with water only. Current-voltage curves confirm that αENACa expressed in oocytes does not produce an amiloride-sensitive Na^+ current.

Discussion

In the present study we have identified two alternatively spliced forms of αENAC, i.e., αENACa and αENACb. Both variants encode truncated proteins with a deletion of amino acids at the carboxyl terminus. One of the alternatively spliced forms, αENACa, was characterized in some detail. Both PCR analysis and RNase protection studies reveal less expression of αENACa in the lung and kidney, compared with αENAC. Like αENAC, transcripts for αENACa are expressed in the taste bud-enriched circumvallate and other

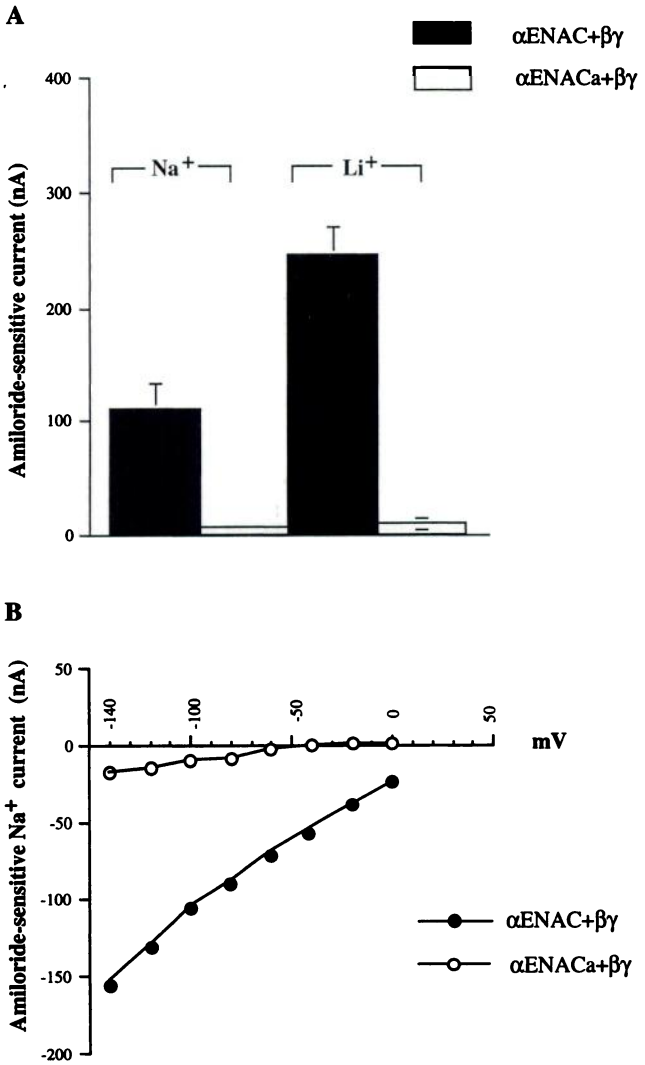

Fig. 8. Expression of αENAC and αENACa in *Xenopus* oocytes. A, Specific amiloride-sensitive Na^+ and Li^+ currents in oocytes coinjected with αENAC or αENACa and β and γ subunit cRNAs. The whole-cell current at −100-mV holding potential was measured in bathing solution containing 100 mM Na^+ or Li^+. In oocytes transfected with αENAC and β and γ subunits, the amiloride-sensitive currents are the difference between the currents before (Na^+, 208 ± 40.4 nA, n = 6; Li^+, 367 ± 62 nA, n = 3, mean ± standard error) and after (Na^+, 87.4 ± 14.3 nA, n = 6; Li^+, 98 ± 20 nA, n = 3, mean ± standard error) addition of 5 μM amiloride to the bathing solution. The currents (<120 nA, n = 5) in oocytes transfected with αENACa and β and γ subunits are not significantly affected by 5 μM amiloride. B, Current-voltage relation of the amiloride-sensitive Na^+ current, obtained under the same conditions as in A.

epithelium of the tongue, consistent with a role in salty taste transduction (10). PCR analysis indicates undetectable expression of αENACa in the lung, relative to the kidney, in contrast to the similar levels in the lung and kidney revealed by RNase protection. Conceivably, in the lung additional alternative splicing hinders detection of a PCR signal for αENACa. Whether the protein expression of αENAC and αENACa corresponds to the transcript expression remains to be determined.

Transfection of αENAC and αENACa into HEK-293 cells leads to an increase in specific [^{3}H]phenamil binding, compared with cells transfected with vector alone. [^{3}H]Phenamil binding in the control HEK-293 cells may reflect endogenous amiloride-binding proteins other than the sodium channel. Lazdunski and co-workers (15) recently showed that the enzyme diamine oxidase binds [^{3}H]phenamil with high affinity and a drug specificity similar to that observed with ENAC. However, diamine oxidase activity was not detected in HEK-293 cells (15). We transfected αENAC into four distinct cell lines, all of which displayed endogenous [^{3}H]phenamil binding and no more than a 2.5–3-fold increase in binding elicited by transfection. The native αENAC in colon and kidney tissues is relative unstable, and its expression can be enhanced by a low-salt diet and steroid treatment (16, 17). A down-regulation mechanism may hinder robust expression of αENAC or αENACa in transfected cells. The substantial expression of αENAC and αENACa in HEK-293 cells allowed us to compare the amiloride-binding properties of the two proteins. The binding profile for αENACa, which lacks the putative second transmembrane portion of the channel, resembles that for αENAC. Functional evaluation of alternatively spliced αENACa in *Xenopus* oocytes shows that this truncated protein does not produce an amiloride-sensitive current, suggesting that the second transmembrane domain is a crucial region for forming a channel pore. It is also possible that the second transmembrane domain of αENAC contributes to the association of the α subunit with β and/or γ subunits that are required for channel activities.

Genetic studies on the degenerin gene *Mec-4* in *C. elegans*, which is homologous to mammalian αENAC, have shown that the second transmembrane domain in Mec-4 and its homologues is critical for channel activities involved in touch sensitivity. Single-amino acid mutations in the second transmembrane domain of Mec-4 alter degeneration of touch neurons, whereas replacement of the second transmembrane domain of mutant Mec-4 with the corresponding region of rat αENAC rescues touch sensitivity (18). These observations, taken together with our findings, favor the conclusion that the second transmembrane domain does contain the ion channel. Our studies of [^{3}H]phenamil binding indicate that the amiloride binding site does not reside on the second transmembrane domain and more likely occurs in the extracellular loop of αENAC. Binding presumably elicits a conformational change of channel structure that blocks Na^+ current. Recently, other reports also suggested that amiloride does not directly plug the Na^+ pore. For instance, use of an anti-amiloride antibody has identified a putative amiloride binding site from residues 278 to 283 (WYRFHY) in αENAC, a region distant from the putative ion channel pore. Deletion of this region diminishes amiloride blockade of Na^+ currents in *Xenopus* oocytes (19).

Identification of alternatively spliced forms of αENAC indicates a heterogeneity of αENAC that may account for the multiple species of proteins observed during purification of this channel (5). The alternatively spliced forms of αENAC may function as regulatory components for ENAC. Because of the critical importance of ways in which the subunits are combined, the alternatively spliced α subunits may substantially influence the channel activity of the multimeric protein.

Acknowledgments

We thank Seth Blackshaw for helpful discussions, Roxanne Ashworth for DNA sequencing, and Nancy Bruce for assistance in preparing the manuscript.

References

1. Garty, H., and D. J. Benos. Characteristics and regulatory mechanisms of the amiloride-blockable Na^+ channel. *Physiol. Rev.* **68:**309–372 (1988).
2. Heck, G. L., S. Mierson, and J. A. DeSimone. Salt taste transduction occurs through an amiloride-sensitive sodium transport pathway. *Science (Washington D. C.)* **223:**403–405 (1984).
3. Avenet, P., and B. Lindemann. Amiloride-blockable sodium currents in isolated taste receptor cells. *J. Membr. Biol.* **105:**245–255 (1988).
4. Schiffman, S. S., E. Lockhead, and F. W. Maes. Amiloride reduces the taste intensity of Na^+ and Li^+ salts and sweeteners. *Proc. Natl. Acad. Sci. USA* **80:**6136–6140 (1983).
5. Benos, D. J., G. Saccomani, and S. Sariban-Sohraby. The epithelial sodium channel: subunit number and location of the amiloride binding site. *J. Biol. Chem.* **262:**10613–10618 (1987).
6. Benos, D. J., G. Saccomani, B. M. Brenner, and S. Sariban-Sohraby. Purification and characterization of the amiloride-sensitive sodium channel from A6 cultured cells and bovine renal papilla. *Proc. Natl. Acad. Sci. USA* **83:**8525–8529 (1986).
7. Canessa, C. M., J. D. Horisberger, and B. C. Rossier. Epithelial sodium channel related to proteins involved in neurodegeneration. *Nature (Lond.)* **361:**467–470 (1993).
8. Lingueglia, E., N. Voilley, R. Waldmann, M. Lazdunski, and P. Barbry. Expression cloning of an epithelial amiloride-sensitive Na^+ channel: a new channel type with homologies to *Caenorhabditis elegans* degenerins. *FEBS Lett.* **318:**95–99 (1993).
9. Canessa, C. M., L. Schild, G. Buell, B. Thorens, I. Gautschi, J. D. Horisberger, and B. C. Rossier. Amiloride-sensitive epithelial Na^+ channel is made of three homologous subunits. *Nature (Lond.)* **367:**463–467 (1994).
10. Li, X. J., S. Blackshaw, and S. H. Snyder. Expression and localization of amiloride-sensitive sodium channels indicate a role for non-taste cells in taste perception. *Proc. Natl. Acad. Sci. USA* **91:**1814–1818 (1994).
11. Wong, P. C., and D. W. Cleveland. Characterization of dominant and recessive assembly-defective mutations in mouse neurofilament NF-M. *J. Cell Biol.* **111:**1987–2003 (1990).
12. Barbry, P., M. Champe, O. Chassande, S. Munemitsu, G. Champigny, E. Lingueglia, P. Maes, C. Frelin, A. Tartar, A. Ullrich, and M. Lazdunski. Human kidney amiloride-binding protein: cDNA structure and functional expression. *Proc. Natl. Acad. Sci. USA* **87:**7347–7351 (1990).
13. Barbry, P., C. Frelin, P. Vigne, E. J. Cragoe, and M. Lazdunski. [^{3}H]Phenamil, a radiolabelled diuretic for the analysis of the amiloride-sensitive Na channels in kidney membrane. *Biochem. Biophys. Res. Commun.* **135:**25–32 (1986).
14. Vigne, P., G. Champigny, R. Marsault, P. Barbry, C. Frelin, and M. Lazdunski. A new type of amiloride-sensitive cationic channel in endothelial cells of brain microvessels. *J. Biol. Chem.* **264:**7663–7668 (1986).
15. Novotny, W. F., O. Chassande, M. Baker, M. Lazdunski, and P. Barbry. Diamine oxidase is the amiloride-binding protein and is inhibited by amiloride analogues. *J. Biol. Chem.* **269:**9921–9925 (1994).
16. Lingueglia, E., S. Renard, R. Waldmann, N. Voilley, G. Champigny, H. Plass, M. Lazdunski, and P. Barbry. Different homologous subunits of the amiloride-sensitive Na^+ channel are differently regulated by aldosterone. *J. Biol. Chem.* **269:**13736–13739 (1994).
17. Pacha, J., G. Frindt, L. Antonian, R. B. Silver, and L. G. Palmer. Regulation of Na channels of the rat cortical collecting tubule by aldosterone. *J. Gen. Physiol.* **102:**25–42 (1993).
18. Hong, K., and M. Driscoll. A transmembrane domain of the putative channel subunit MEC-4 influences mechanotransduction and neurodegeneration in *C. elegans*. *Nature (Lond.)* **367:**470–473 (1994).
19. Lin, C., R. T. Eaton, T. Kicber-Emmons, C. M. Canessa, B. C. Rossier, D. G. Eaton, and T. R. Kleyman. Mutagenesis of a putative amiloride-binding site of the epithelial Na^+ channel, in *Proceedings of the Symposium on Epithelial Na Channels and Mechanosensitive Channels*. Switzerland, 9 (1994).

Send reprint requests to: Solomon H. Snyder, Johns Hopkins School of Medicine, Department of Neuroscience, 725 N. Wolfe St., Baltimore, MD 21205.